JACS
JOURNAL OF THE AMERICAN CHEMICAL SOCIETY
Article
pubs.acs.org/JACS

Development of Large Band-Gap Conjugated Copolymers for Efficient Regular Single and Tandem Organic Solar Cells

Kai Li, Zuojia Li, Kui Feng, Xiaopeng Xu, Lingyan Wang, and Qiang Peng*

Key Laboratory of Green Chemistry and Technology of Ministry of Education, College of Chemistry, Sichuan University, 29 Wangjiang Road, Chengdu 610064, China

Supporting Information

ABSTRACT: We demonstrated the synthesis and characterization of two conjugated copolymers, **PBDTFBZO** and **PBDTFBZS**, consisting of dialkylthiol substituted benzo[1,2-*b*:4,5-*b*′]dithiophene donor and monofluorinated benzotriazole acceptor blocks. The resulting copolymers show large band gaps, deep HOMO and LUMO energy levels. Improved V_{oc}, J_{sc}, and FF were obtained at the same time to increase overall efficiencies of their single and tandem polymer solar cells. The enhanced V_{oc} can be ascribed to a low-lying HOMO energy level by incorporating dialkylthiol and fluorine substituents on the polymer backbone. The improvement in J_{sc} and FF are likely due to high carrier mobility, suppressed charge recombination, and fine nanostructure morphology. A 7.74% PCE was achieved from the regular single device based on **PBDTFBZS**:$PC_{71}BM$ blend film with 3% 1,8-diiodooctane (DIO) additive. In combination with low band gap diketopyrrolopyrrole (DPP)-based copolymer, tandem devices based on **PBDTFBZS** exhibited high PCE up to 9.40%. The results indicate that **PBDTFBZO** and **PBDTFBZS** are promising polymer donor materials for future application of large-area polymer solar cells.

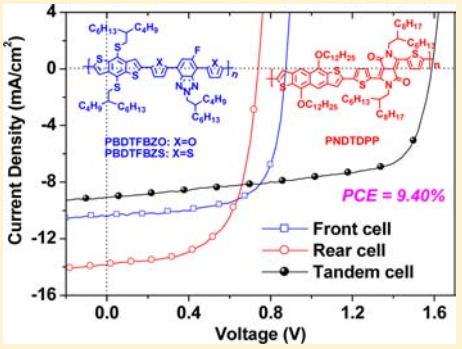

1. INTRODUCTION

Polymer solar cells (PSCs) have attracted wide attention as a promising clean and renewable energy resource because of their unique advantages for achieving lightweight, low-cost, large-area, and flexible devices through inkjet printing and roll to roll solution processes.[1−3] In the past decade, rapid and significant progress has been made in this field, and the power conversion efficiencies (PCEs) of PSCs have reached from around 1% to over 10%, particular due to optimization of material band gaps, carrier mobilities, energy levels, and nanoscale morphologies of active networks.[4−8] Further improvement of PCE is still required for commercialization. The influencing factors of PCE include the open-circuit voltage (V_{oc}), short-circuit current density (J_{sc}), and fill factor (FF). V_{oc} is proportional to the offset between the highest occupied molecular orbital (HOMO) of polymeric donor and the lowest unoccupied molecular orbital (LUMO) of the fullerene acceptor.[9] Therefore, the use of a conjugated polymer with low-lying HOMO energy level could be an effective way to achieve high V_{oc} values in photovoltaic devices.[10] J_{sc} is controlled by all of the favorable effect factors for light absorption enhancement and transfer, and the FF value is influenced by the charge carrier mobility, charge recombination, and nanoscale morphology of the photoactive layer.[11−13] High mobility polymer donors with conjugated side chains[14−17] and low band gap conjugated copolymers[17−21] were carefully designed for realization of high J_{sc} values. The blend morphology could be well controlled with the help of some solvent additives, such as 1,8-diiodooctane (**DIO**) and 1-chloronaphthalene (**CN**).[22−24] Thus, the design of new efficient photovoltaic polymers must consider many parameters, such as optical band gap, absorption coefficient, charge carrier mobility, charge recombination, morphology, and so on. However, the reported polymeric materials comprising all of these factors are presently unknown.

Among the various conjugated polymers, alternating copolymers based on dialkoxyl-substituted benzo[1,2-*b*:4,5-*b*′]dithiophene (**BDT**) units have attracted considerable interest as electron-donating building blocks in PSC application.[25] Exceptional photovoltaic performances were achieved by using these copolymers, with high PCEs of more than 6%.[12,26] The structural modification with thienyl side chains was further performed on the BDT skeleton, and many copolymers were designed and synthesized for highly efficient PSCs.[18,20,27] Very recently, dialkylthiol-substituted BDT homopolymer was developed with deeper HOMO energy level resulting in high V_{oc} of up to 0.99 V.[28] Another interesting strategy to improve the V_{oc} is to attach fluorine (F) atoms to the conjugated backbone, especially the electron-deficient units of donor (D)-acceptor (A) copolymers.[4,29−35] Our previous work has proven that this approach can simultaneously lower both the HOMO and LUMO energy levels, while having just minor effect on the optical band gap.[20] The fluorination is also beneficial to J_{sc} and FF, which can be attributed to the fluorine atom-induced high carrier mobilities, suppressed charge

Received: June 25, 2013
Published: August 20, 2013

   dx.doi.org/10.1021/ja406220a | *J. Am. Chem. Soc.* 2013, 135, 13549−13557

Scheme 1. Synthetic Routes to PBDTFBZO and PBDTFBZS[a]

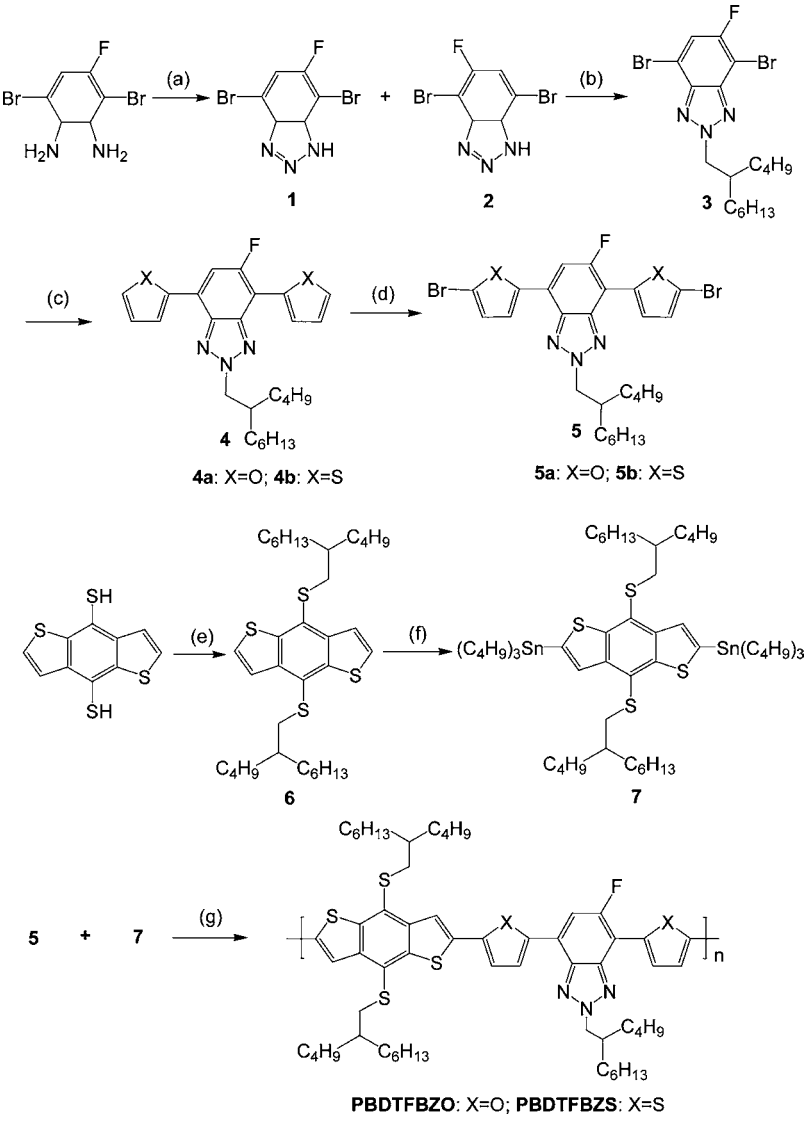

[a]Reagents and conditions: (a) $NaNO_2$, AcOH; (b) 2-butyl-1-octylbromide, *t*-BuOK, EtOH, 20%; (c) 2-tributylstannylthiophene or 2-tributylstannylfuran, $Pd(PPh_3)_2Cl_2$, THF, for **4a**, 92%; for **4b**, 90%; (d) NBS, $CHCl_3$, AcOH, for **5a**, 73%; for **5b**, 70%; (e) 2-butyl-1-octylbromide, K_2CO_3, DMSO, 42%; (f) *n*-butyllithium, *n*-tributyltin chloride, THF, 93%; (g) Pd_2dba_3, P(*o*-tolyl)$_3$, toluene, 110 °C, for **PBDTFBZO**, 65%; for **PBDTFBZS**, 62%.

recombination, as well as specific nanoscale morphology of active blends.[4,19,20,29−35]

To enhance the overall performance of PSCs, the parameters of V_{oc}, J_{sc} and FF must be improved simultaneously according to the equation PCE = $(J_{sc}V_{oc}FF)/P_{in}$, where P_{in} is the input light power. However, the PCE of single junction PSCs is challenging and limited at around 8% using a bulk heterojunction (BHJ) device structure.[8,12,29,36−40] In this type of cell, photons with energy smaller than the band gap and photons with larger energy will lose at the same time.[41] The concept of tandem solar cells was then put forward to reduce these losses, which involved a double-junction or multijunction subcell with different active layers, each absorbing different parts of the solar spectrum.[42−44] The PCE of a tandem PSC was predicted by theoretical modeling to be up to 14%.[45] Actually, the PCE records of PSCs in the past 10 years were kept and refreshed by tandem devices.[3,7,46,47] In this work, we designed and synthesized two novel D−A copolymers made up of dialkylthiol-substituted BDT and monofluorinated benzotriazole, **PBDTFBZO** and **PBDTFBZS** (Scheme 1), which exhibit high V_{oc}, J_{sc}, and FF at the same time, giving rise to high PCE values up to 7.74% even in regular single-junction devices. As a comparison, the related photovoltaic data of the reported high-performance PSCs based on copolymers of benzo[1,2-*b*:4,5-*b*′]dithiophene and benzotriazole are listed in Table 1. Because the N lone pair on benzotriazole unit is more basic (donating) than an O/S lone pair, **PBDTFBZO** and **PBDTFBZS** show large band gaps and low-lying HOMO and LUMO energy levels. Although the optical responses are not so satisfactory in comparison with low band gap (LGB) conjugated copolymers, large band gaps show potential and important application in tandem PSCs. Incorporating these benzotriazole-based copolymers and our previously reported diketopyrrolopyrrole (**DPP**)-based copolymer (**PNDTDPP**),[48] typical double-junction tandem PSCs were fabricated, and high PCEs of up to 9.4% were achieved.

dx.doi.org/10.1021/ja406220a | J. Am. Chem. Soc. 2013, 135, 13549−13557

Table 1. Photovoltaic Data of Some Reported High-Performance PSCs Based on Copolymers of Benzo[1,2-*b*:4,5-*b*′]dithiophene and Benzotriazole

polymer	V_{oc} (V)	J_{sc} (mA/cm^2)	FF (%)	PCE (%)	ref
PBnDTHTAZ	0.70	11.14	55.2	4.30	19
PBnDTFTAZ	0.79	11.83	72.9	7.10	19
PBDTHBTA	0.58	7.41	56.5	2.43	34
PBDTFBTA	0.75	11.90	67.2	6.00	34
PBDTTDTBTz	0.54	9.47	60.6	3.10	35
PBDTFBZO	0.91	11.81	58.2	6.25	this work
PBDTFBZS	0.88	12.36	71.2	7.74	this work

2. RESULTS AND DISCUSSION

2.1. Synthesis and Characterization. Synthetic routes to the monomers and copolymers are described in Scheme 1. Monofluorinated benzotriazole was used as a new acceptor because the monofluorinated electron-deficient substitutions show more unique properties in PSC application than difluorinated ones in recent work.[20,49−51] The new monofluorinated benzotriazole derivative was prepared by alkylation and cyclization reactions using 4-fluoro-1,2-phenylenediamine as a starting material, which could be easily obtained by previous methods.[20,49−51] Furan[23,24] and thiophene[19,34] groups were attached on both sides of the above benzotriazole skeleton to isolate the donors and acceptors for reducing the steric hindrance, which was helpful to improve the planarity and $\pi-\pi$ stacking of polymer backbones. **PBDTFBZO** and **PBDTFBZS** were subsequently prepared by Stille coupling polymerization in good yields, using a $Pd_2dba_3/P(o\text{-tolyl})_3$ catalytic system. The structures of copolymers were determined with ^{1}H NMR spectroscopy and elemental analysis, which is consistent with the proposed structures. Both copolymers are soluble in common chlorinated organic solvents, such as chloroform, chlorobenzene, and *o*-dichlorobenzene. The molecular weight and polydispersity index (PDI) were determined by gel permeation chromatography (GPC) with calibration against polystyrene standards. The number average molecular weights (M_n) of **PBDTFBZO** and **PBDTFBZS** were found to be 48.3 and 39.6 kDa, with PDIs of 2.2 and 1.9, respectively. The obtained high molar masses and narrow polydispersity are generally helpful to improve PSC performance by enhancing J_{sc} and FF.[3] The thermal stability of the copolymers was investigated by thermogravimetric analysis (TGA), which showed that **PBDTFBZO** and **PBDTFBZS** had good thermal stabilities with decomposition temperatures (5% weight loss) of 346 and 342 °C, respectively. Obviously, the thermal stability of these polymers is adequate for their applications in PSC devices.

2.2. Optical Properties and Electrochemical Study. The optical properties of the two copolymers were investigated by UV−vis absorption spectroscopy. The absorption spectra of **PBDTFBZO** and **PBDTFBZS** in chloroform solutions and thin solid films are shown in Figure 1a and b. Relevant data are summarized in Table 2. Clearly, the solution and film absorptions of the two polymers exhibit similar well-defined absorption behaviors, which indicated that they are favorable to form the ordered arrangement and densely packed state to obtain high carrier mobility and photovoltaic performance. This strong $\pi-\pi$ stacking properties were also verified by the observed vibronic shoulders in thin films at about 600 nm. When the polymer solutions were heated to 80 °C, the absorption peaks were slightly blue-shifted (Figure 1a and b) compared to those determined from the solution at room temperature, which indicated strong aggregation even in solution and partial disaggregation of the polymer backbone at high temperatures. The polymer films also exhibited red-shifted and well-defined absorption spectra with the edges at 678 and 684 nm for **PBDTFBZO** and **PBDTFBZS**, corresponding to optical band gaps of 1.83 and 1.81 eV, respectively. **PBDTFBZO** with furan units has a slightly larger band gap than **PBDTFBZS** with thiophene units, which proves that the thiophene can efficiently increase the conjugation length.

Highest-occupied (HOMO) and lowest-unoccupied molecular orbital (LUMO) energy levels of the polymers are crucial for the selection of appropriate acceptor materials in active blends in PSCs. Cyclic voltammetry (CV) was employed to evaluate the electrochemical properties and electronic energy levels of the copolymers. CV measurements were carried out on a CHI660 potentiostat/galvanostat electrochemical workstation at a scan rate of 50 mV s^{-1},[16] with a platinum wire counter electrode and an Ag/AgCl reference electrode in anhydrous nitrogen-saturated 0.1 mol L^{-1} acetonitrile (CH_3CN) solution of tetrabutylammonium perchlorate (Bu_4NClO_4). A Pt plate coated with a thin film of the studied copolymer, a Pt wire, and an Ag/AgCl (0.1 M) were used as the work electrode, counter electrode, and reference electrode, respectively. The energy level of the Ag/AgCl reference electrode was calibrated against the ferrocene/ferrocenium (Fc/Fc^+) system to be 4.40 eV in this work.[16,52] As shown in Figure 2a, both polymers show reversible oxidation and reduction behaviors. The onsets of oxidation and reduction of **PBDTFBZO** were observed at

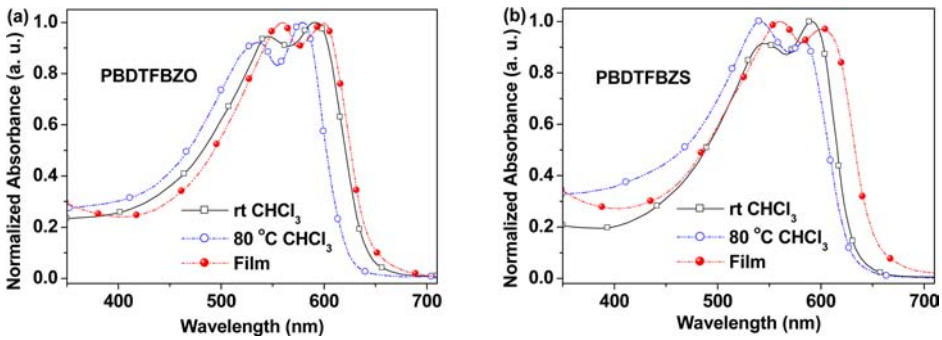

Figure 1. UV−vis absorption spectra of **PBDTFBZO** (a) and **PBDTFBZS** (b) in chloroform solutions at room temperature and 80 °C and in thin solid films.

dx.doi.org/10.1021/ja406220a | J. Am. Chem. Soc. 2013, 135, 13549−13557

Table 2. Absorption Spectral Properties and Molecular Energy Level Data of the Polymers

polymer	solution λ_{max} (nm) rt	solution λ_{max} (nm) 80 °C	film λ_{max}(nm)	E_g^{opt} (eV)	HOMO (eV)	LUMO (eV)	E_g^{CV} (eV)
PBDTFBZO	545, 591	535, 579	560, 600	1.83	−5.38	−3.28	2.10
PBDTFBZS	540, 584	546, 592	562, 603	1.81	−5.32	−3.26	2.06

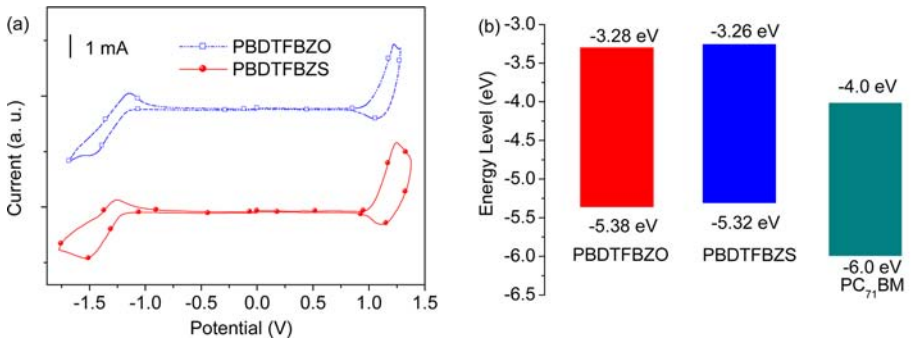

Figure 2. Cyclic voltammograms (a) and HOMO and LUMO energy levels (b) of **PBDTFBZO** and **PBDTFBZS**.

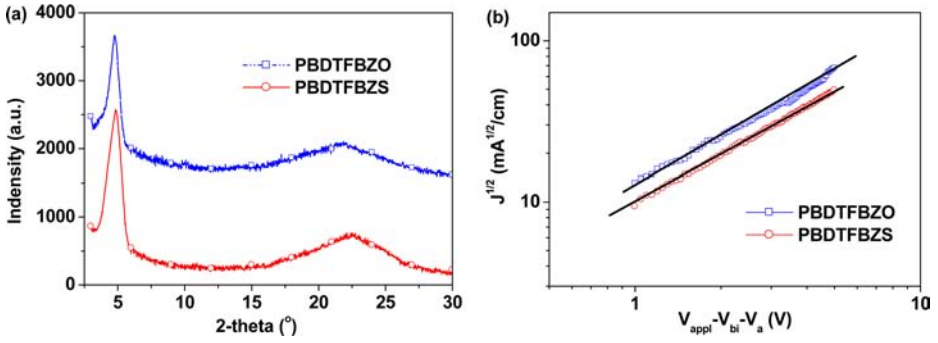

Figure 3. (a) X-ray diffraction patterns of **PBDTFBZO** and **PBDTFBZS** films on silicon wafers. (b) $J^{1/2}-V$ characteristics of **PBDTFBZO** and **PBDTFBZS** hole-only devices measured at ambient temperature.

+0.98 and −1.12 V vs Fc/Fc^+, corresponding to HOMO and LUMO levels at −5.38 and −3.28 eV. For **PBDTFBZS**, the onsets were observed at +0.92 and −1.14 V, corresponding to HOMO and LUMO levels at −5.32 and −3.26 eV. The values indicated that the resulting polymers had deep HOMO energy levels compared to those copolymers of dialkoxyl-substituted BDT and difluorinated benzotriazole,[19] which were expected to obtain higher V_{oc} values in PSC applications. The electron density of furan is lower than that of thiophene due to the higher ionization potential.[53] Thus, by replacing the thiophene with a furan moiety, the HOMO level of **PBDTFBZO** was found to be lower than that of **PBDTFBZS**, which will lead to further improving the V_{oc} value. In order to make a clear comparison, the electronic energy level diagram of **PBDTFBZO**, **PBDTFBZS**, and $PC_{71}BM$ is described in Figure 2b. The LUMO gap of 0.72−0.74 eV and HOMO gap of 0.62−0.68 eV between the copolymers and $PC_{71}BM$ are large enough to overcome the intrachain exciton binding energy and thus guarantee efficient exciton dissociation and transfer.[54]

To better understand the effect of furan and thiophene linkers on the electronic structures of **PBDTFBZO** and **PBDTFBZS**, molecular simulation on D−A model compounds was performed through Density Functional Theory (DFT) calculations at the B3LYP/6-31G* level of theory by using the Gaussian 09 program suite.[16] To make the calculation time reasonable, the alkyl groups were replaced by methyl groups because they do not significantly affect the equilibrium geometries or electronic properties.[16] The resulting theoretical HOMO and LUMO level positions are illustrated in Supplementary Figure S1. Ab initio calculation indicates that they favor planar conformations, which enables the electrons to be delocalized across the whole backbones for high carrier mobility. The results show that both HOMO frontier orbitals extend across the entire conjugated systems from donor to acceptor sections. Because the electronegativity of oxygen is stronger than that of sulfur, the HOMO frontier orbital of the model compound with a furan linker distributes more on the side of benzotriazole. Compared with HOMO, HOMO-1 orbitals are mainly on the benzo[1,2-*b*:4,5-*b*′]dithiophene units, which indicates that internal charge transfer is possible and the transfer trend is more evident in the model compound with a thiophene linker. This is consistent with the fact that the band gap of **PBDTFBZS** is smaller than that of **PBDTFBZO**. Although the LUMO orbitals also extend across the entire conjugated systems, the electron density is mainly localized on the benzotriazole segment for both model compounds. This is different from the result of a low band gap copolymer, whose LUMO is almost completely delocalized on the acceptor skeleton with strong electron-withdrawing power.[16]

2.3. X-ray Diffraction and Hole Mobility. To gain deeper insight of the crystallinity and molecular stacking of the copolymers, X-ray diffraction (XRD) analysis of the copolymer films was performed (Figure 3a). The distinct primary strong peaks (100) at ca. 2θ = 4.78° and 4.83° were related to the

dx.doi.org/10.1021/ja406220a | J. Am. Chem. Soc. 2013, 135, 13549−13557

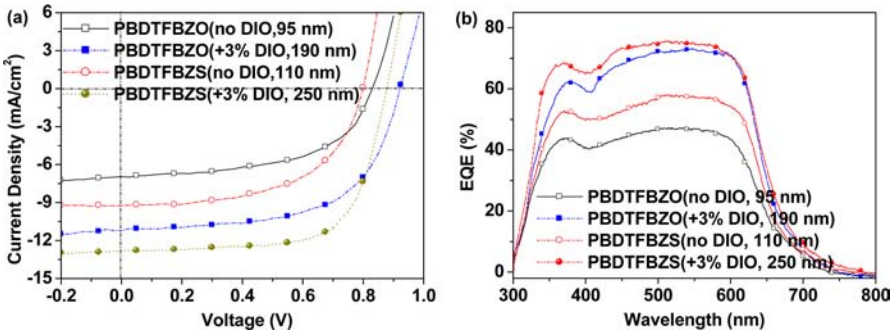

Figure 4. (a) $J-V$ curves of copolymer/$PC_{71}BM$-based regular single solar cells under AM 1.5 G illumination, 100 mW/cm^2. (b) EQE curves of copolymer/$PC_{71}BM$-based regular single solar cells.

Table 3. Photovoltaic Properties of the PSCs Based on Copolymer/$PC_{71}BM$ (1:2, w/w) under AM 1.5G, 100 mW/cm^2

polymer	DIO (%)	thickness (nm)	V_{oc} (V)	J_{sc} (mA/cm^2)	FF (%)	PCE_{max}/PCE_{ave} (%)
PBDTFBZO	no	95	0.82	7.23	53.6	3.18/2.92
PBDTFBZO	3	140	0.85	9.55	57.4	4.66/4.31
PBDTFBZO	3	190	0.91	11.81	58.2	6.25/5.96
PBDTFBZO	3	230	0.92	10.79	57.0	5.66/5.30
PBDTFBZO	3	310	0.88	9.21	55.5	4.50/4.24
PBDTFBZS	no	110	0.78	9.13	57.6	4.10/3.76
PBDTFBZS	3	130	0.83	11.54	62.7	6.01/5.83
PBDTFBZS	3	200	0.86	11.85	68.3	6.96/6.69
PBDTFBZS	3	250	0.88	12.36	71.2	7.74/7.42
PBDTFBZS	3	320	0.85	12.03	65.6	6.71/6.54

polymer lamellar spacing, corresponding to a d-spacing of 18.46 and 18.27 Å for **PBDTFBZO** and **PBDTFBZS**, respectively. As expected, these two values are almost the same because the side chains on aromatic polymer backbones are not changed in these two copolymers. The (010) diffraction peak has a broad feature located at ca. $2\theta = 21.8°$ and 22.5°, corresponding to a face to face packing distance of 4.07 and 3.95 Å for **PBDTFBZO** and **PBDTFBZS**, respectively. Both copolymers showed clear $\pi-\pi$ stacking, which can be attributed to the increased inter- or intramolecular interactions from F−H, F−F interactions. Because the electron-donating nature, S−S and F−S interaction from thiophene linkers can extend π-conjugation and induce larger planar structure of aromatic backbone,[55] **PBDTFBZS** exhibits a shorter cofacial distance than **PBDTFBZO**. Thus, **PBDTFBZS** is expected to have higher mobility than polymer **PBDTFBZO**, which is favorable for enhanced carrier transport, larger J_{sc} and high PCE in PSCs. This was further supported by the hole mobility measurements using the space charge limited current (SCLC) model. The $J-V$ characteristics are plotted in Figure 3b. As shown in Figure 3b, **PBDTFBZS** has relatively higher hole mobility of 4.3×10^{-3} cm^2 V^{-1} s^{-1} compared with 2.6×10^{-3} cm^2 V^{-1} s^{-1} for **PBDTFBZO**, which indicates the sulfur-rich thiophene linkers help to enhance the mobility than furan linkers attributed to the S−S and other interactions associated with the sulfur atoms, resulting in good planarity and $\pi-\pi$ stacking feature.[55]

2.4. Regular Single Solar Cell Performance. To demonstrate the potential application of the two conjugated polymers **PBDTFBZO** and **PBDTFBZS** in PSCs, regular single devices were first fabricated from the resulting copolymers and [6,6]-phenyl-C_{71}-butyric acid methyl ester ($PC_{71}BM$) with a typical device structure of ITO/PEDOT:PSS/copolymer:$PC_{71}BM$/Ca/Al. In this work, poly(3,4-ethylenedioxythiophene) (PEDOT):poly(styrenesulfonate) (PSS) was used to facilitate the hole extraction. $PC_{71}BM$ was selected because it could complement the absorption well in the visible region.[56] Detailed processes for device fabrication and characterizations were described in Supporting Information. The performance of PSCs was strongly affected by the processing parameters, such as the choice of solvent, the use of additives, blend ratio, and thickness of the copolymer and $PC_{71}BM$. The active layers were spin-coated from an o-dichlorobenzene (DCB) solution of the donor polymers and acceptor. For PSCs based on **PBDTFBZO** and **PBDTFBZS**, the ratio of polymer to $PC_{71}BM$ was adjusted from 1:1 to 1:4 (w/w); the optimized weight ratio between the copolymer and $PC_{71}BM$ is 1:2. 1,8-Diiodooctane (DIO) was used as a processing additive to optimize the morphology of the active blends. The current density−voltage ($J-V$) curves and device performance data are also presented in Figure 4a and Table 3.

As shown in Figure 4a, without any postfabrication treatment, **PBDTFBZO** and **PBDTFBZS** devices exhibited moderate PCEs of 3.18% and 4.10%. Polymer **PBDTFBZO** exhibited a V_{oc} of 0.82 V, 0.04 V higher than that of **PBDTFBZS**, which can be attributed to the lower-lying HOMO energy level. However, higher photocurrents, better fill factor, and enhanced device performance were obtained from polymer **PBDTFBZS**. The J_{sc} of PSCs is affected by many factors, including the absorption properties (absorption range and coefficient) of the blending layer and the charge carrier mobility. The better absorption and higher hole mobility of **PBDTFBZS** are expected to be responsible for those enhancements, as discussed above. When we incorporated 3% DIO additive to the blend solutions by volume, the device performances were improved very much, which can be attributed to the increased J_{sc} value and well-controlled nanoscale morphology of the BHJ films. The overall efficiencies were also dependent on the thickness of the copoly-

dx.doi.org/10.1021/ja406220a | J. Am. Chem. Soc. 2013, 135, 13549−13557

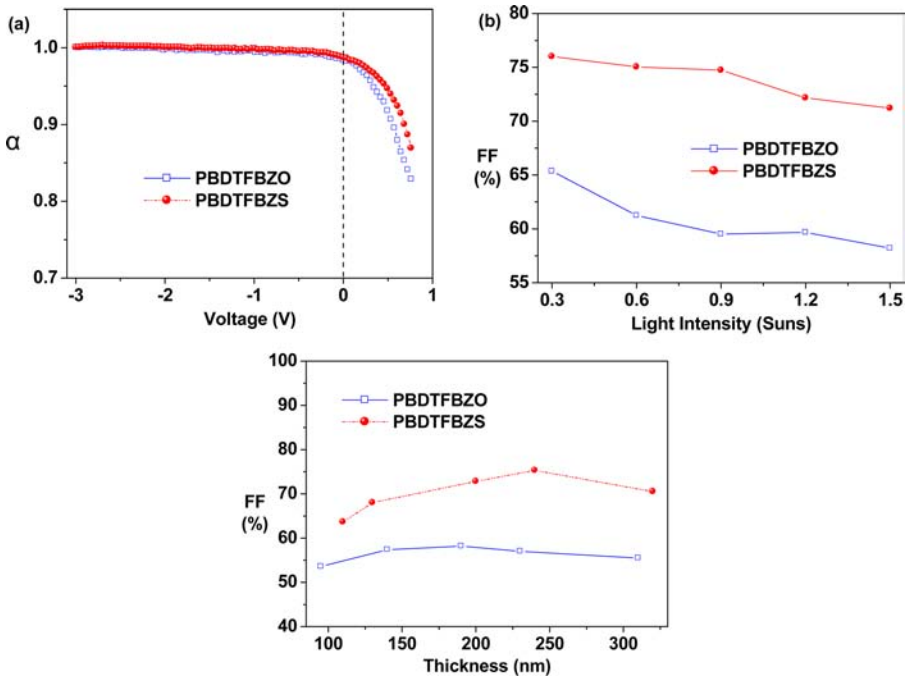

Figure 5. (a) Scaling exponent vs voltage for **PBDTFBZO**/$PC_{71}BM$ (190 nm)- and **PBDTFBZO**/$PC_{71}BM$ (200 nm)-based devices. (b) FF vs light intensity for **PBDTFBZO**/$PC_{71}BM$ (190 nm)- and **PBDTFBZO**/$PC_{71}BM$ (250 nm)-based devices. (c) The effect of film thickness on the FF values of the active layers of the regular **PBDFBZO** and **PBDTFBZS** devices.

mer:$PC_{71}BM$ blend layers. Around the optimized thickness of 190 nm, **PBDTFBZO** device showed high PCE of 6.25% with V_{oc} = 0.91 V, J_{sc} =11.81 mA/cm^2, and FF = 58.2%. The best device from these regular single PSCs was obtained from a 240 nm blend of **PBDTFBZS**:$PC_{71}BM$ in 1:2 weight ratio and afforded high PCE of 7.74%, with V_{oc} = 0.88 V, J_{sc} =12.36 mA/cm^2, and FF = 71.2%. The PCE value of 7.74% is still very competitive because it is obtained just in a conventional single device. From above, it is intriguing to note that high V_{oc} values were obtained in these single PSCs due to the deep HOMO energy levels of these polymers by incorporation of dialkylthiol-substituted BDT donors and monofluorinated benzotriazole acceptors. The FF of 71.2% is the top high value in present regular single PSCs, which indicated that no significant carrier recombination loss occurs within the active layer with the aid of DIO additive. To evaluate the accuracy of the measurements, external quantum efficiencies (EQE) of the devices with or without DIO additive were measured and are shown in Figure 4b. The shapes of the EQE curves of the devices based on copolymer:$PC_{71}BM$ are similar to their absorption spectra, which indicates that most of the absorbed photons of the copolymers contribute to the photocurrent generation. Broad response ranges covering 300−700 nm were obtained with average EQEs of 47% and 58% within this region for **PBDTFBZO** and **PBDTFBZS**, respectively, without DIO additive. The EQEs were significantly improved to 73% and 76% for the **PBDTFBZO**:$PC_{71}BM$ (1:2) and **PBDTFBZS**:$PC_{71}BM$ (1:2) device upon the addition of 3% DIO. All of the J_{sc} values calculated by integrating the EQE curves with an AM 1.5 G reference spectrum are within 5% error compared to the corresponding J_{sc} values obtained from the $J-V$ curves. The highest EQE of about 76% for **PBDTFBZS** induced the highest J_{sc} of 12.36 mA/cm^2, which was in agreement with the integrated J_{sc} of 12.41 mA/cm^2.

2.5. Bimolecular Recombination and Film Morphology. In order to determine the loss mechanisms causing the noted FF differences, we used a bimolecular recombination model and measured the photovoltaic performance under varied light intensity from 0.3 to 1.5 suns.[33,57,58] This measurement technique is regarded as a simple way to examine bimolecular recombination of free charges that can limit the photocurrent. If the bimolecular recombination is minimized, more and more charge carriers can be easily collected and the photocurrent should scale linearly with the light intensity. Therefore, a sublinear scaling of the photocurrent with light intensity would predict that a fraction of the charge carriers are lost during transport due to the process of bimolecular recombination.[33,57,58] As shown in Figure 5a, α value became larger with increasing applied voltage and internal electric field. Clearly, there is relatively low bimolecular recombination even at short circuit because $\alpha \approx 1$. **PBDTFBZS** shows the larger α value, indicating the lower carrier recombination loss compared to that of **PBDTFBZO**. This reduction in bimolecular recombination was also observed with light intensity (Figure 5b) and film thickness (Figure 5c). **PBDTFBZS** showed a higher absolute FF value under different film thickness and variable light intensity. As shown in Figure 5b, **PBDTFBZS** exhibits an insensitivity of FF compared to **PBDTFBZO**-based devices, which indicates an efficient suppression recombination and avoidance of FF losses. Despite the effect of fluorine substituent atoms, thiophene linkers are more able to stifle recombination and avoid FF losses than are furan moieties. Thus, **PBDTFBZS** have enhanced overall device performance by improving the values of V_{oc}, J_{sc}, and FF simultaneously.

To better understand the PSC performance of the present materials, the microstructures and morphology of the copolymer/$PC_{71}BM$ active layers were investigated by transmission electron microscopy (TEM) for the blend films processed with and without the DIO additive. Figure 6 shows

dx.doi.org/10.1021/ja406220a | J. Am. Chem. Soc. 2013, 135, 13549−13557

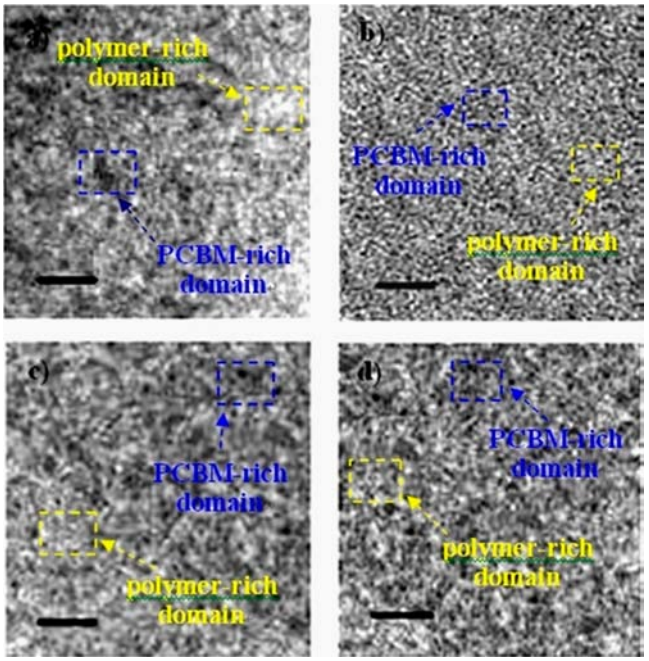

Figure 6. TEM images of **PBDTFBZO**/$PC_{71}BM$ and **PBDTFBZS**/$PC_{71}BM$ without DIO (a, b) and with 3% DIO (c, d). Scale bar =200 nm. DIO = 1,8-diiodooctane.

TEM images of copolymer/$PC_{71}BM$ blend films. Because fullerene derivatives have higher electron densities compared to polymer donors, $PC_{71}BM$ scatters electrons more efficiently from the electronic beam.[59] Therefore, the dark areas in the TEM images are attributed to $PC_{71}BM$-rich domains, and the bright regions to the polymer-rich domains. It is clear that the DIO additive has a positive effect for promoting the demixing of the polymer and $PC_{71}BM$ and inducing the formation of good nanoscale structures. When the blend films were processed with 3% DIO, both TEM images of **PBDTFBZO** and **PBDTFBZS** films possess significantly more homogeneous morphologies, suggesting well-controlled nanoscale phase separation. Since the limited diffusion length of excitons is about 10 nm, smaller or larger domain size will result in reduced charge carrier generation and a concomitant loss of photocurrent. The reason is that space charge accumulation caused by sluggish charge carriers can induce a nonuniform electric field, which decreases the photocurrent with strong electric field dependence and subsequently results in low FF value.[60] As shown in Figure 6, optimized nanoscale phase separation was achieved by adding 3% DIO as additives for the **PBDTFBZS**/$PC_{71}BM$ (1:2) blend. The results agreed well with the improvement of J_{sc} from 9.13 to 12.36 mA/cm^2 for the PSC measurements. The well-ordered nanoscale morphology of **PBDTFBZS**/$PC_{71}BM$ should also result in high charge carrier mobility, which gives rise to higher FF of 71.2% and better device performance with a PCE up to 7.74%.

2.6. Inverted Tandem Solar Cell Performance. The regular single solar cell performance was not easily improved further because **PBDTFBZO** and **PBDTFBZS** exhibited no longer absorption band over 700 nm. Considering our previously reported diketopyrrolopyrrole (**DPP**)-based copolymer (**PNDTDPP**) (Figure 7a),[48] it is clear to see that these two copolymers complementarily cover the solar spectrum from 300 to 1000 nm and the overlap is small (Figure 7b), which encouraged us to fabricate tandem cells with a inverted structure of ITO/ZnO/**PBDTFBZS**:$PC_{71}BM$/PEDOT:PSS/ZnO/**PNDTDPP**:$PC_{71}BM$/MoO_3/Ag.[3,7] In this work, a large band gap polymer **PBDTFBZS** combined with $PC_{71}BM$ are selected as front cell active materials, and the low band gap polymer **PNDTDPP** with $PC_{71}BM$ are selected as the rear cell

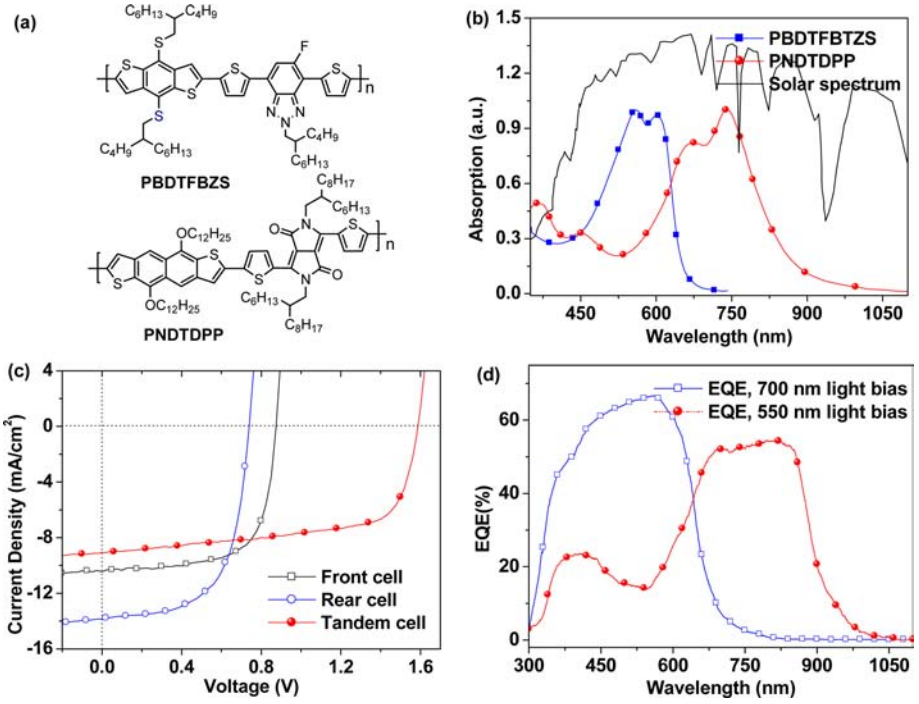

Figure 7. (a) Molecular structures of **PBDTFBZS** and **PNDTDPP**. (b) Absorption spectra of **PBDTFBZS** and **PNDTDPP** and solar spectrum. (c) *J*–*V* curves of the front (**PBDTFBZS**:$PC_{71}BM$) and rear (**PNDTDPP**:$PC_{71}BM$) subcells under AM 1.5 G illumination, 100 mW/cm^2. (d) EQE curve of the tandem device. A 700 nm and a 550 nm light are used to obtain front and rear cell EQE, respectively.

dx.doi.org/10.1021/ja406220a | J. Am. Chem. Soc. 2013, 135, 13549–13557

active materials. ZnO thin film was used as the electron transport layer, and PEDOT:PSS and MoO_3 were employed as the hole transport layer for the front and rear cells, respectively. The $J-V$ characteristics of the single junction and tandem cells are depicted in Figure 7c.

The **PBDTFBZS**:$PC_{71}BM$ and **PNDTDPP**:$PC_{71}BM$ cells showed good performance with 6.18% and 6.35% PCE, respectively. The detailed parameters of these single cells are summarized in Table 4. The EQE curves of

Table 4. Photovoltaic Properties of the Inverted Tandem PSCs Based on Copolymer/$PC_{71}BM$ (1:2, w/w) under AM 1.5 G, 100 mW/cm^2

devices	V_{oc} (V)	J_{sc} (mA/cm^2)	FF (%)	PCE (%)
front cell	0.88	10.44	67.2	6.18
rear cell	0.74	13.86	61.9	6.35
tandem cell	1.59	9.10	65.0	9.40

PBDTFBZS:$PC_{71}BM$ and **PNDTDPP**:$PC_{71}BM$ are shown in Figure 7d. The front cell with large band gap polymer (**PBDTFBZS**:$PC_{71}BM$) showed relatively high quantum efficiency from 300 to 750 nm, with maximum EQE of 65% at about 560 nm. Its integrated J_{sc} was calculated to be 10.5 mA/cm^2. The rear cell based on **PNDTDPP** had a broad photoresponse from 300 to 1000 nm. The maximum EQE is 54% at ca. 800 nm, and EQE is over 50% from 670 to 860 nm. From the EQE curve, its integrated J_{sc} was 9.0 mA/cm^2. For the tandem device, it showed a V_{oc} of 1.59 V, J_{sc} of 9.1 mA/cm^2, FF of 65%, and the PCE is 9.40%. The high photovoltaic performance achieved by using these two polymers with different absorption bands can be attributed to the simultaneous enhancement of V_{oc}, J_{sc}, and FF. The V_{oc} is almost equal to the sum of single junction cells' V_{oc}, indicating the effectiveness of the interconnection layer.[3,7,61] Tandem solar cells' current is usually determined by the subcells with the lowest J_{sc}. Therefore, the measured J_{sc} of 9.1 mA/cm^2 is very close to the integrated J_{sc} of 9.0 mA/cm^2 from the rear cell.[3,7,62,63] If the photocurrents from both subcells are almost equal, the FF of the tandem cell will be the average of the individual cells.[63] Our tandem cell shows a higher FF than the average for either of the two subcells, which is in accordance with the results from other tandem cells.[3,7,61]

3. CONCLUSIONS

In conclusion, we have demonstrated, for the first time, designation and synthesis of two D−A conjugated copolymers, **PBDTFBZO** and **PBDTFBZS**, consisting of dialkylthiol-substituted BDT donor and monofluorinated benzotriazole acceptor moieties. The prepared copolymers show good absorptions and deep HOMO and LUMO energy levels, as well as high hole mobility. Improved V_{oc}, J_{sc}, and FF were obtained at the same time, giving rise to overall efficiencies in the fabricated single and tandem PSCs. A high power conversion efficiency of 7.74% was achieved from the regular single device based on **PBDTFBZS**:$PC_{71}BM$ blend film with 3% DIO additive. In combination with DPP-based polymer **PNDTDPP**, tandem PSCs showed high PCEs up to 9.4%. Consequently, the design strategy has been proven to be a feasible and successful approach to develop efficient photovoltaic polymers, and **PBDTFBZO** and **PBDTFBZS** are promising polymer donors for future commercial application of large-area regular single and tandem PSCs.

■ ASSOCIATED CONTENT

Supporting Information

Experimental details on materials and methods, synthesis of monomers and polymers, hole mobility measurement, device fabrication. Theoretical calculation results and ^{1}H NMR spectra of the monomers and copolymers. This material is available free of charge via the Internet at http://pubs.acs.org.

■ AUTHOR INFORMATION

Corresponding Author

qiangpengjohnny@yahoo.com

Notes

The authors declare no competing financial interest.

■ ACKNOWLEDGMENTS

This work was supported by the NSFC (20802033, 21272164), the 863 Project (2013AA031901), the Youth Science and Technology Foundation of Sichuan Province (2013JQ0032), the Program for New Century Excellent Talents in University (NCET-10-0170), and the Fundamental Research Funds for the Central Universities (2012SCU04B01, YJ2011025).

■ REFERENCES

(1) Thompson, B. C.; Fréchet, J. M. J. *Angew. Chem., Int. Ed.* **2008**, *47*, 58.
(2) Cheng, Y. J.; Yang, S. H.; Hsu, C. S. *Chem. Rev.* **2009**, *109*, 5868.
(3) Dou, L.; You, J.; Yang, J.; Chen, C. C.; He, Y.; Murase, S.; Moriarty, T.; Emery, K.; Li, G.; Yang, Y. *Nat. Photonics* **2012**, *6*, 180.
(4) Zhou, H.; Yang, L.; Stuart, A. C.; Price, S. C.; Liu, S.; You, W. *Angew. Chem., Int. Ed.* **2011**, *50*, 2995.
(5) Chu, T. Y.; Lu, J.; Beaupré, S.; Zhang, Y.; Pouliot, J. R.M.; Wakim, S.; Zhou, J.; Leclerc, M.; Li, Z.; Ding, J.; Tao, Y. *J. Am. Chem. Soc.* **2011**, *133*, 4250.
(6) Amb, C. M.; Chen, S.; Graham, K. R.; Subbiah, J.; Small, C. E.; So, F.; Reynolds, J. R. *J. Am. Chem. Soc.* **2011**, *133*, 10062.
(7) You, J. B.; Dou, L. T.; Yoshimura, K.; Kato, T.; Ohya, K.; Moriarty, T.; Emery, K.; Chen, C. C.; Gao, J.; Li, G.; Yang, Y. *Nat. Commun.* **2013**, *4*, 1446.
(8) Small, C. E.; Chen, S.; Subbiah, J.; Amb, C. M.; Tsang, S. W.; Lai, T. H.; Reynolds, J. R.; So, F. *Nat. Photonics* **2012**, *6*, 115.
(9) Dennler, G.; Scharber, M. C.; Ameri, T.; Denk, P.; Forberich, K.; Waldauf, C.; Brabec, C. J. *Adv. Mater.* **2008**, *20*, 579.
(10) Peng, Q.; Park, K.; Lin, T.; Durstock, M.; Dai, L. M. *J. Phys. Chem. B* **2008**, *112*, 2801.
(11) Peet, J.; Kim, J. Y.; Coates, N. E.; Ma, W. L.; Moses, D.; Heeger, A. J.; Bazan, G. C. *Nat. Mater.* **2007**, *6*, 497.
(12) Liang, Y. Y.; Xu, Z.; Xia, J. B.; Tsai, S. T.; Wu, Y.; Li, G.; Ray, C.; Yu, L. P. *Adv. Mater.* **2010**, *22*, E135.
(13) Li, G.; Shrotriya, V.; Huang, J.; Yao, Y.; Moriarty, T.; Emery, K.; Yang, Y. *Nat. Mater.* **2005**, *4*, 864.
(14) Hou, J. H.; Tan, Z. A.; Yan, Y.; He, Y. J.; Yang, C. H.; Li, Y. F. *J. Am. Chem. Soc.* **2006**, *128*, 4911.
(15) Huang, F.; Chen, K. S.; Yip, H. L.; Hau, S. K.; Acton, O.; Zhang, Y.; Luo, J.; Jen, A. K. Y. *J. Am. Chem. Soc.* **2009**, *131*, 13886.
(16) Peng, Q.; Lim, S. L.; Wong, I. H.; Xu, J.; Chen, Z. K. *Chem.—Eur. J.* **2012**, *18*, 12140.
(17) Peng, Q.; Fu, Y. Y.; Liu, X. J.; Xu, J.; Xie, Z. Y. *Polym. Chem.* **2012**, *3*, 2933.
(18) Huo, L. J.; Hou, J. H.; Zhang, S. Q.; Chen, H. Y.; Yang, Y. *Angew. Chem., Int. Ed.* **2010**, *49*, 1500.
(19) Price, C. S.; Stuart, A. C.; Yang, L. Q.; Zhou, H. X.; You, W. *J. Am. Chem. Soc.* **2011**, *133*, 4625.
(20) Peng, Q.; Liu, X. J.; Su, D.; Fu, G. W.; Xu, J.; Dai, L. M. *Adv. Mater.* **2011**, *23*, 4554.
(21) Chang, C. Y.; Cheng, Y. J.; Hung, S. H.; Wu, J. S.; Kao, W. S.; Lee, C. H.; Hsu, C. S. *Adv. Mater.* **2012**, *24*, 549.

(22) Wang, E. G.; Ma, Z. F.; Zhang, Z.; Vandewal, K.; Henriksson, P.; Inganäs, O.; Zhang, F. L.; Andersson, M. R. *J. Am. Chem. Soc.* **2011**, *133*, 14244.
(23) Woo, C. H.; Beaujuge, P. M.; Holcombe, T. W.; Lee, O. P.; Fréchet, J. M. J. *J. Am. Chem. Soc.* **2011**, *132*, 15547.
(24) Yiu, A. T.; Beaujuge, P. M.; Lee, O. P.; Woo, C. H.; Michael, F.; Toney, M. F.; Fréchet, J. M. J. *J. Am. Chem. Soc.* **2012**, *134*, 2180.
(25) Hou, J. H.; Park, M. H.; Zhang, S. Q.; Yao, Y.; Chen, L. M.; Li, J. H.; Yang, Y. *Macromolecules* **2008**, *41*, 6012.
(26) Yuan, M. C.; Chiu, M. Y.; Chiang, C. M.; Wei, K. H. *Macromolecules* **2010**, *43*, 6270.
(27) Li, X. H.; Choy, W. C. H.; Huo, L. J.; Xie, F. X.; Sha, W. E. I.; Ding, B. F.; Guo, X.; Li, Y. F.; Hou, J. H.; You, J. B.; Yang, Y. *Adv. Mater.* **2012**, *24*, 3046.
(28) Lee, D.; Stone, S. W.; Ferraris, J. P. *Chem. Commun.* **2011**, *47*, 10987.
(29) Chen, H. Y.; Hou, J.; Zhang, S.; Liang, Y.; Yang, G.; Yang, Y.; Yu, L.; Wu, Y.; Li, G. *Nat. Photonics* **2009**, *3*, 649.
(30) Son, H. J.; Wang, W.; Xu, T.; Liang, Y.; Wu, Y.; Li, G.; Yu, L. *J. Am. Chem. Soc.* **2011**, *133*, 1885.
(31) Tumbleston, J. R.; Stuart, A. C.; Gann, E.; You, W.; Ade, H. *Adv. Funct. Mater.* **2013**, *27*, 3463.
(32) Albrecht, S.; Janietz, S.; Schindler, W.; Frisch, J.; Kurpiers, J.; Kniepert, J.; Inal, S.; Pingle, P.; Fostiropoulos, K.; Koch, N.; Neher, D. *J. Am. Chem. Soc.* **2012**, *134*, 14932.
(33) Stuart, A. C.; Tumbleston, J. R.; Zhang, H. X.; Li, W. T.; Liu, S. B.; Ade, H.; You, W. *J. Am. Chem. Soc.* **2013**, *135*, 1806.
(34) Min, J.; Zhang, Z. G.; Zhang, S. Y.; Li, Y. F. *Chem. Mater.* **2012**, *24*, 3247.
(35) Liu, B.; Chen, X. W.; He, Y. H.; Li, Y. F.; Xu, X. J.; Xiao, L.; Li, L. D.; Zou, Y. P. *J. Mater. Chem. A* **2013**, *1*, 570.
(36) He, Z. C.; Zhong, C. M.; Huang, X.; Wong, W. Y.; Wu, H. B.; Chen, L. W.; Su, S. J.; Cao, Y. *Adv. Mater.* **2011**, *23*, 4636.
(37) Collins, B. A.; Li, Z.; Tumbleston, J. R.; Gann, E.; McNeill, C. R.; Ade, H. *Adv. Energy Mater.* **2013**, *3*, 65.
(38) Amb, C. M.; Chen, S.; Graham, K. R.; Subbiah, J.; Small, C. E.; So, F.; Reynolds, J. R. *J. Am. Chem. Soc.* **2011**, *133*, 10062.
(39) Hendriks, K. H.; Heintges, G. H. L.; Gevaerts, V. S.; Wienk, M. M.; Janssen, R. A. J. *Angew. Chem., Int. Ed.* **2013**, *52*, 8341.
(40) Cabanetos, C.; El Labban, A.; Bartelt, J. A.; Douglas, J. D.; Mateker, W. R.; Fréchet, J.M. J.; McGehee, M. D.; Beaujuge, P. M. *J. Am. Chem. Soc.* **2013**, *135*, 4656.
(41) Würfel, W. *Physics of Solar Cells*; Wiley-VCH Verlag GmbH & Co. KGaA: Weinheim, 2005.
(42) Xue, J.; Uchida, S.; Rand, B. P.; Forrest, S. R. *Appl. Phys. Lett.* **2004**, *85*, 5757.
(43) Wang, X. H.; Koleilat, G. I.; Tang, J.; Liu, H.; Kramer, I. J.; Debnath, R.; Brzozowski, L.; Barkhouse, D. A. R.; Levina, L.; Hoogland, S.; Sargent, E. H. *Nat. Photonics* **2011**, *5*, 480.
(44) Riede, M.; Uhrich, C.; Widmer, J.; Timmreck, R.; Wynands, D.; Schwartz, G.; Gnehr, W.-M.; Hildebrandt, D.; Weiss, A.; Hwang, J.; Sundarraj, S.; Erk, P.; Pfeiffer, M.; Leo, K. *Adv. Funct. Mater.* **2011**, *21*, 3019.
(45) Dennler, G.; Scharber, M. C.; Brabec, C. J. *Adv. Mater.* **2009**, *21*, 1323.
(46) Kim, J. Y.; Lee, K.; Coates, N. E.; Moses, D.; Nguyen, T. Q.; Dante, M.; Heeger, A. J. *Science* **2007**, *317*, 222.
(47) Li, W. W.; Furlan, A.; Hendriks, K. H.; Wienk, M. M.; Janssen, R. A. J. *J. Am. Chem. Soc.* **2013**, *135*, 5529.
(48) Peng, Q.; Huang, Q.; Hou, X. B.; Chang, P. P.; Xu, J.; Deng, S. J. *Chem. Commun.* **2012**, *48*, 11452.
(49) Zhang, Y.; Chien, S. C.; Chen, K. S.; Yip, H. L.; Sun, Y.; Davies, J. A.; Chen, F. C.; Jen, A. K. Y. *Chem. Commun.* **2011**, *47*, 11026.
(50) Zhang, Y.; Zou, J. Y.; Cheuh, C. C.; Yip, H. L.; Jen, A. K. Y. *Macromolecules* **2012**, *45*, 5427.
(51) Schroeder, B. C.; Huang, Z.; Ashraf, R. S.; Smith, J.; D'Angelo, P.; Watkins, S. E.; Anthopoulos, T. D.; Durrant, J. R.; McCulloch, I. *Adv. Funct. Mater.* **2012**, *22*, 1663.
(52) Li, Y. F.; Cao, Y.; Gao, J.; Wang, D. L.; Yu, G.; Heeger, A. J. *Synth. Met.* **1999**, *99*, 243.
(53) Bijleveld, J. C.; Zoombelt, A.; Mathijssen, S. G. J.; Wienk, M. M.; Turbiez, M.; de Leeuw, D. M.; Janssen, R. A. J. *J. Am. Chem. Soc.* **2009**, *131*, 16616.
(54) Brabec, C. J.; Winder, C.; Sariciftci, N. S.; Hummelen, J. C.; Dhanabalan, A.; van Hal, P. A.; Janssen, R. A. J. *Adv. Funct. Mater.* **2002**, *12*, 709.
(55) Irvin, J. A.; Schwendeman, I.; Lee, Y.; Abboud, K. A.; Reynolds, J. R. *J. Polym. Sci., Part A: Polym. Chem.* **2001**, *39*, 2164.
(56) Wiek, M. M.; Kroon, J. M.; Verhees, W. J. H.; Knol, J.; Hummelen, J. C.; van Hal, P. A.; Janssen, R. A. J. *Angew. Chem., Int. Ed.* **2003**, *42*, 3371.
(57) Koster, L. J. A.; Mihailetchi, V. D.; Blom, P. W. M. *Appl. Phys. Lett.* **2006**, *88*, 052104.
(58) Shuttle, C. G.; O'Regan, B.; Ballantyne, A. M.; Nelson, J.; Bradley, D. D. C.; Durrant, J. R. *Phys. Rev. B* **2008**, *78*, 113201.
(59) Park, S. H.; Roy, A.; Beaupre, S.; Cho, S.; Coates, N.; Moon, J. S.; Moses, D.; Leclerc, M.; Lee, K.; Heeger, A. J. *Nat. Photonics* **2009**, *3*, 297.
(60) Mihailetchi, V. D.; Wildeman, J.; Blom, P. W. M. *Phys. Rev. Lett.* **2005**, *94*, 126602.
(61) Ameri, T.; Dennler, G.; Lungenschmied, C.; Brabec, C. J. *Energy Environ. Sci.* **2009**, *2*, 347.
(62) Gilot, J.; Wienk, M. M.; Janssen, R. A. J. *Adv. Mater.* **2010**, *22*, E67.
(63) Burdick, J.; Glatfelter, T. *Sol. Cells* **1986**, *18*, 301.